



## Novel Superhydrophobic Cement-based Materials Achieved by Construction of Hierarchical Surface Structure with FAS/SiO<sub>2</sub> Hybrid Nanocomposites

Pengkun Hou,<sup>1,\*</sup> Ran Li,<sup>1</sup> Qinfei Li,<sup>1</sup> Na Lu,<sup>2</sup> Kejin Wang,<sup>3</sup> Mingle Liu,<sup>4</sup> Xin Cheng,<sup>1,\*</sup> and Surendra Shah<sup>1,5</sup>

This work aims at developing novel superhydrophobic cement concrete by applying a tridecafluorooctyltriethoxysilane/nanosilica (FAS/SiO<sub>2</sub>) hybrid nanocomposite onto surfaces of hardened concrete. The hybrid nanocomposite was synthesized and characterized using TEM, TGA and NMR. The performance of the FAS/SiO<sub>2</sub> treated cement paste/mortar samples were evaluated using a water contact angle (WCA) test, lab-raining detachment test, 3D image analysis, and UV irradiation test. The results indicate that the core-shell spherical structured composite had a particle size of about 200 nm and shell thickness of about 50 nm, displayed high pozzolanic reactivity, and enable to polymerize C-S-H gel of the concrete, thus lowering surface energy and modifying surface structure. The WCA of the FAS/SiO<sub>2</sub> treated-concrete samples was larger than 150°, signifying a superhydrophobicity. The FAS/SiO<sub>2</sub> hybrid composite had superior anti-detachment performance, proposing that the treated concrete surface would have a long-term high water-proofing performance. A hierarchical structure observed from the 3D image analysis might be primarily responsible for the increase in the hydrophobicity of the hardened cement-based materials. The 800-hour UV irradiation test results suggested a good stability of superhydrophobicity under severe weathering conditions. It is concluded that the FAS/SiO<sub>2</sub> hybrid nanocomposite has a great potential for improving durability of existing concrete structures.

**Keywords:** Cement-based materials; Core-shell nanocomposite; Hydrophobicity; Surface treatment; Hierarchical structure

**Received** 26 August 2018, **Accepted** 12 October 2018

**DOI:** 10.30919/esmm5f125

### 1 Introduction

Severe deterioration may happen when concrete structures are subjected to aggressive or harsh environments. Consequently, this could result in the service life of field structures far shorter than that originally designed.<sup>1,2</sup> Improving longevity of concrete structures not only can save costs for maintenances and repairs but also help increase greenability and sustainability of concrete infrastructures. Concrete, even before being subjected to any mechanical and environmental loading, has abundant interconnected capillary voids and pre-existing microcracks, and it is permeable. Water, having a molecular size of 0.275 nm, can penetrate into very tiny voids/cracks of pristine concrete, and it also serves as a carrier bringing various corrosive agents (e.g., deicing chemicals) into concrete.<sup>3, 4</sup> Thus,

chemical and physical reactions (e.g., wetting-drying, freezing-thawing, sulfate attack, and corrosion damages) can occur in concrete<sup>5,6</sup> and lead to deterioration of the concrete. Thus, keeping water away from concrete is a critical and effective way of reducing concrete deterioration.<sup>7</sup>

The apparent water contact angle (WCA) has been widely used to characterize the water-repellent properties of various solid materials. When WCA is greater than 90°, the material is often considered having a hydrophobic surface. When WCA is greater than 150°, the material is considered having a superhydrophobic surface.<sup>8</sup> That is, the higher the WCA value, the greater hydrophobicity or water-repellence the material will have.

Generally, there are two ways to achieve superhydrophobicity: reducing surface energy and enhancing surface roughness.<sup>9</sup> Organic agents, such as silane, siloxane and silicones have often been used for concrete surface treatment so as to acquire a low surface energy. However, use of the technique of increasing the surface roughness to achieve superhydrophobicity of cementitious materials has rarely been reported. Recently, Liu et al.<sup>10</sup> innovatively increased the surface roughness of cement pastes by using a polymer as a negative template to copy the hierarchical structure of lotus leaf, and they enabled the cement pastes to gain the identical hierarchical structure and achieved superhydrophobicity. However, this method can only be applied to fresh cement-based materials rather than to existing hardened cement-based materials.

Reduction of the surface material porosity through a surface treatment is another way of reducing the ingress of corrosive

<sup>1</sup>Shandong Provincial Key Lab for the Preparation and Measurement of Building Materials, Jinan, Shandong, 250022, China

<sup>2</sup>Lyles School of Civil Engineering, Purdue University, West Lafayette, Indiana, 47906, USA

<sup>3</sup>Department of Civil, Construction and Environmental Engineering, Iowa State University, Ames, IA 50011, USA

<sup>4</sup>Shenzhen Gangchuang Building Material Co., Ltd, Shenzhen, Guangdong, 518000, China

<sup>5</sup>Department of Civil and Environmental Engineering, Northwestern University, Evanston, IL, 60201, USA

\*E-mail: pkhou@163.com; chengxin@ujn.edu.cn

agents into the inner matrix. The reactive silica-based agents, such as  $\text{Na}_2\text{SiO}_3$ , has long been used due to their in-situ reaction with the surface concrete, forming extra amount of C-S-H gel and densifying the surface concrete microstructure.<sup>11</sup> More recently, other organic and inorganic silica-based material, such as tetraethoxysilane (TEOS) and colloidal nanosilica, have been found effective in densifying the microstructure of surface concrete through their particle filling effect and high pozzolanic reactivity, thus altering the transport properties of the cement concrete.<sup>12-14</sup>

In the present study, both techniques of the surface energy reduction and surface microstructure densification were adapted in the development of a novel superhydrophobic material, hybridized from the tridecafluorooctyltriethoxysilane (FAS) and nano-silica ( $\text{nSiO}_2$ ). This FAS/ $\text{SiO}_2$  (organic/inorganic) hybridized nanocomposite, having synergized superhydrophobicity, was then used for the surface treatment of cement-based materials. Such a hybridization was based on a fact that the fluorine-containing materials used in the hybrid nanocomposite possess a low surface energy, and they can transfer their hydrophobic properties to the surface of the applied concrete effectively. The  $\text{nSiO}_2$  in the hybrid composite can offer a hierarchical structure layer to the applied concrete surfaces and lead to an increase in the surface roughness of the concrete. In addition, the  $\text{nSiO}_2$  can also react with calcium hydroxide ( $\text{Ca(OH)}_2$  or CH) in the substrate cement paste or mortar, and such a pozzolanic can help improve the bond and compatibility of the hybrid nanocomposite with the treated concrete. Together, these mechanisms of improvements have led to a synergized performance of the FAS/ $\text{SiO}_2$  nanocomposite treated concrete.

## 2 Materials and Methods

### 2.1 Materials

#### 2.1.1 Nanocomposite

The chemicals used for nanocomposite included tridecafluorooctyl triethoxysilane (here after FAS) with a purity of 95%, ethanol and ammonium hydroxide (28 wt.% concentration), and tetraethoxysilane (here after TEOS) with a purity of 98% and a density of 0.931-0.934  $\text{g/cm}^3$ . (Note,  $\text{nSiO}_2$  was the hydrolysis product of the TEOS.)

#### 2.1.2 Cement-based substrates

Both cement paste and mortar substrates were studied. The cement used was ordinary Portland cement 42.5 complying to Chinese standard GB 175-2007. The sand used for mortar was a river sand with the fineness modulus of 2.8.

### 2.2 Sample preparation

#### 2.2.1 Synthesis of FAS/ $\text{SiO}_2$ nanocomposite

A multi-step synthesizing protocol was used. First, solution A was made by<sup>15</sup> dissolving FAS (0.5 mL) and TEOS (5 mL), at a target FAS/ $\text{SiO}_2$  ratio of 3/7, in 25 mL ethanol, and the solution was stirred for 30 minutes to achieve a good dispersion. Next, solution B was prepared by dissolving 6ml 28%  $\text{NH}_3 \cdot \text{H}_2\text{O}$  in 25 ml ethanol. Then, solution A was poured into solution B, and they were stirred at the speed of 600 rpm at a room temperature for 12 hours. Finally, this obtained milky mixture was ultrasonicated for 30 min before being used for the surface treatment of cement-based substrates. For a comparison, individual FAS and  $\text{nSiO}_2$  were also used to treat the surfaces of cement-based substrates separately, and the treated samples were named as FAS and NS, respectively.

To characterize the pure hybrid nanocomposite, the synthesized solutions were firstly centrifuged and then triple-centrifuged with

ethanol. The remaining were then oven-dried at 40 °C for 24 hours before being used for chemical analyses.

#### 2.2.2 Preparation of paste and mortar samples

The 4 cm×4 cm×4 cm mortar samples, with a water-to-cement ratio (w/c) of 0.55 and the cement-to-sand ratio (c/s) of 0.33, were prepared. They were demolded one day after casting and then cured in a standard curing chamber (21 °C, 95% RH). After 6 months of curing, the hardened mortar samples were sliced into a size of 4 cm×4 cm×2 cm before being treated with nanocomposite.

The 2 cm×2 cm×2 cm paste samples with w/c=0.38 were prepared. They were demolded and cured under the same condition as the mortar samples for 6 months before being treated with the nanocomposite.

#### 2.2.3 Surface treatment of paste and mortar samples

Before surface treatment, mortar and paste samples were vacuum-dried at 60 °C for 24 hrs to avoid the influence of moisture on treatment.

After drying, two different surface treatment methods were employed: spraying and immersion. When spraying was used, a surface treatment agent, such as a hybrid FAS/ $\text{SiO}_2$  nanocomposite, was sprayed onto the top surfaces for 3 times at the interval of 10 minutes. During each spray, the saturated surface was achieved. The treated samples were denoted as H-Spray. When immersion was used, samples were immersed into hybrid FAS/ $\text{SiO}_2$  nanocomposite solutions for 10 or 60 minutes, labeled as H-I-10 and H-I-60, respectively.

After surface treatment, the samples were then cured in standard curing conditions (21 °C, 95% RH) for another 3 days before being characterized.

### 2.3 Evaluation on the reactivity of treatment agents

One of the critical concerns for applying a surface treatment agent on to a hardened cementitious material is its detachment, which governs the effectiveness and longevity of the treated material.<sup>16</sup> When the FAS/ $\text{SiO}_2$  hybrid composite is applied onto concrete,  $\text{nSiO}_2$  in the composite can react with CH on the surface of the treated concrete materials (i.e., pozzolanic reaction), and the resulting C-S-H gel can improve the bond between the FAS/ $\text{SiO}_2$  composite and the treated concrete, thus increasing the resistivity of detachment.

To assess such a pozzolanic reactivity, the chemical reactions between different treatment agents (FAS/ $\text{SiO}_2$  hybrid nanocomposite and  $\text{nSiO}_2$ ) and hardened concrete materials were simulated in the present study. During the simulation process, CH or C-S-H gel was mixed with a FAS/ $\text{SiO}_2$  hybrid nanocomposite at the mass ratio of 4:1 and a water-to-binder (CH or C-S-H gel) ratio of 2.0. The blend was then dispersed using ultrasonication for 15 minutes. After sonication, the samples were sealed in glass vials, and their CH content were assessed using a thermogravimetric analysis (TGA) at different reaction times.

To evaluate the reactivity of the hybrid nanocomposite with C-S-H gel, pure C-S-H gel was synthesized using a low hydrothermal method according to the previous study.<sup>17,18</sup> The C-S-H synthesis was conducted with the following steps:

- (1) Calcining  $\text{CaCO}_3$  into CaO at 1000 °C for 5 h;
- (2) Mixing the obtained CaO and nanosilica (from Aladdin) to form a blend at a C/S ratio of 1.5 and 1.0;

- (3) Adding water to the blend to form a mixture at a water-to-blend ratio of 2.0 ;
- (4) Agitating the mixture at 100 rpm for 30 minutes to form a slurry; and
- (5) Hydrothermal treating the resulting slurry at 120 °C for 3 days in a reactor.

## 2.4 Characterization of surface treated mortar and paste samples

### 2.4.1 Water absorption and weathering

The water absorption characteristics of the mortar and pastes studied were evaluated according to the ASTM C1585-13 Standard Test Method for Measurement of Rate of Absorption of Water by Hydraulic-Cement Concretes.

To determine the anti-detachment of the treatment agents from the cement-based materials, the water absorption characteristics and hydrophobicity of samples before and after lab-simulated raining were evaluated. The water flow speed of simulation was 420 mL/min.

### 2.4.2 Static water contact angle (WCA) and UV aging test

The static WCA was measured using a JC2000D3X contact angle goniometer (Shanghai Zhongchen Digital Technology Apparatus Co. Ltd, China). Ten points of three specimens were chosen randomly, and the representative value was an average value of these points. To evaluate their hydrophobicity, surface treatment agents, FAS and FAS/SiO<sub>2</sub> in the present study, were first dispersed in ethanol solvents, and the solutions were then dropped on separate glass slides. After the solvent evaporates, the WCAs of the glass surfaces treated by FAS and FAS/SiO<sub>2</sub> was measured.

The durability of hybrid treatment agent against UV aging was accessed by measuring the water contact angles after UV light (500 W) irradiation. The intensity of UV light striking on the surface of tested samples was 0.17 mW/cm<sup>2</sup>.

### 2.4.3 Morphology study

TEM observations of FAS-SiO<sub>2</sub> hybrid materials were carried out using JEM-1011 transmission electron microscopy. The Zeiss EVO LS 15 SEM was used for morphological investigations of the cement pastes before and after surface treatment.

### 2.4.4 Thermalgravimetry analysis (TGA)

TGA was used to determine the chemical/mineral compositions of the hybrid composite/blends according to different decomposition

temperatures of different constituents. The amount of FAS in an FAS-SiO<sub>2</sub> hybrid nanocomposite and the CH content in a blend of FAS-SiO<sub>2</sub>/SiO<sub>2</sub>/FAS-CH-H<sub>2</sub>O with time were determined by a thermogravimetry analyzer (TGA/DSC 1, Mettler, Swiss). During the test, samples were heated in argon atmosphere at 20 °C/min to a different temperature range, depending upon the sample preparation method and the nature of the tested materials (30 °C to 700 °C for the hybrid materials, and 50 °C to 900 °C for blended binders).

### 2.4.5 Nuclear magnetic resonance (NMR)

To characterize the effects of the treatment agents on the molecule structure of the C-S-H gel, the evolution of the C-S-H gel was traced by the single-pulse NMR spectra on Agilent 600 spectrometer with operational frequencies for <sup>29</sup>Si of 119.15 MHz employing a spinning speed of 6.0 kHz. Cement paste samples made with w/c of 0.38 and cured for 6 months were vacuum dried for a surface treatment. After the surface treatment, they were cured for another 3 days. Then, powder samples at the surface of the paste samples were collected and tested using NMR.

### 2.4.6 3D image metrology

The surface roughness of the hardened cement paste sample before and after surface treatment was monitored using a 3D optical profiler (S neoxSensofar, Spain) in focus-variation mode. To get a relatively smooth surface, cement pastes were casted in petri dishes and cured for 28 days. Samples were then treated by different agents before testing. The average roughness (Ra) and mean distance between peaks (Rsm) were calculated in 26 individual assays according to the ISO 4287.<sup>19</sup>

Table 1 summarizes all material variables and test methods used in the present study.

## 3. Results and discussions

### 3.1 Characteristics of the FAS/SiO<sub>2</sub> hybrid nanocomposite

TGA was used to investigate the phase compositions of FAS/SiO<sub>2</sub> hybrid nanocomposite. The first derivative curve of the TGA result, DTG curve, was made following Kim's work,<sup>20</sup> and the result is shown in Fig. 1.

Three main stages can be seen in Fig. 1 resulting from the decompositions of three different phases in the hybrid FAS/SiO<sub>2</sub> nanocomposite. The mass loss in stage I (below 200 °C) could be mainly due to the dehydration and dihydroxylation of the nanoparticles. There was a little mass loss in stage II (200 - 300 °C),

**Table 1** Summary of all the materials variables and test methods.

Sample	Paste (w/c=0.38)	Mortar (w/c=0.55)	CH-FAS/nSiO <sub>2</sub>	C-S-H-FAS/nSiO <sub>2</sub>
Water absorption ratio		√		
Water contact angle	√			
Morphology	√			
Surface roughness	√			
Pozzolanic reactivity/TGA			√	
Molecule structure /NMR				√
Lab simulated weathering		√		



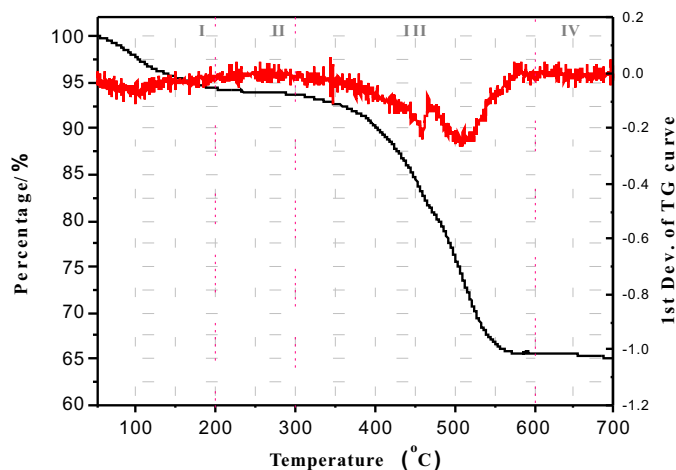


Fig. 1 TGA and DTG curves of FAS/SiO<sub>2</sub> hybrid composite.

which could be ascribed to the desorption of the physically adsorbed FAS since the boiling temperature of FAS is 220 °C.<sup>21, 22</sup> A significant mass loss occurred in stage III (300 - 600 °C), which signified the decomposition of chemically bounded FAS to the nSiO<sub>2</sub> particles.<sup>23</sup> Based on the results, it can be deduced that very little FAS was physically adsorbed, and most FAS was chemically bounded on nSiO<sub>2</sub> particles of the hybrid FAS/SiO<sub>2</sub> nanocomposite. Based on the weight loss percentage of the tested sample, FAS in the hybrid nanocomposite can be calculated as 29.97%, which is very close to the designed value of 30%.

The morphology of the hybrid FAS/SiO<sub>2</sub> nanocomposite was examined using Transmission Electron Microscope (TEM). It can be seen in Figs. 2a&b that the hybrid FAS-SiO<sub>2</sub> nanocomposite appeared as a core-shell like material with a diameter of approximately 200 nm and a shell thickness of about 50 nm. The SiO<sub>2</sub> modified with FAS was further analyzed using TEM-EDS mapping, and the results are presented in Figs. 2c&d. Figs. 2c illustrates that the F element distributed evenly with silicon and oxide. Fig. 2d shows that the F/Si ratio of the hybrid particle was relatively higher at the locations of 20 - 65 nm and 150 - 200 nm along the diameter of the particle studied. This verified the shell of the particle with a shell thickness of about 50 nm.

In summary, the above characterization study suggests that the FAS/ SiO<sub>2</sub> hybrid composite that was synthesized in the present study consisted of core-shell nanoparticles with a core diameter of approximately 200 nm and a shell thickness of about 50 nm, and these particles were formed by FAS chemically bounded on the surfaces of nSiO<sub>2</sub>.

### 3.2 Properties of the FAS-SiO<sub>2</sub> hybrid nanocomposite

#### 3.2.1 Pozzolanic reactivity

As mentioned previously, the detachment resistance of the FAS/SiO<sub>2</sub> hybrid composite (a surface treatment agent) on the treated concrete surface was evaluated based on the pozzolanic reactivity of the FAS/SiO<sub>2</sub> hybrid composite. The pozzolanic reactivity of the FAS/SiO<sub>2</sub> hybrid composite was evaluated using TGA on simulated samples made with the FAS/SiO<sub>2</sub> hybrid composite CH and H<sub>2</sub>O. Fig. 3a shows the TGA test result of the FAS/SiO<sub>2</sub>-CH-H<sub>2</sub>O sample in a comparison with nSiO<sub>2</sub>-CH-H<sub>2</sub>O sample at an age of 3 days. Fig. 3b shows how the remaining CH in a tested sample was

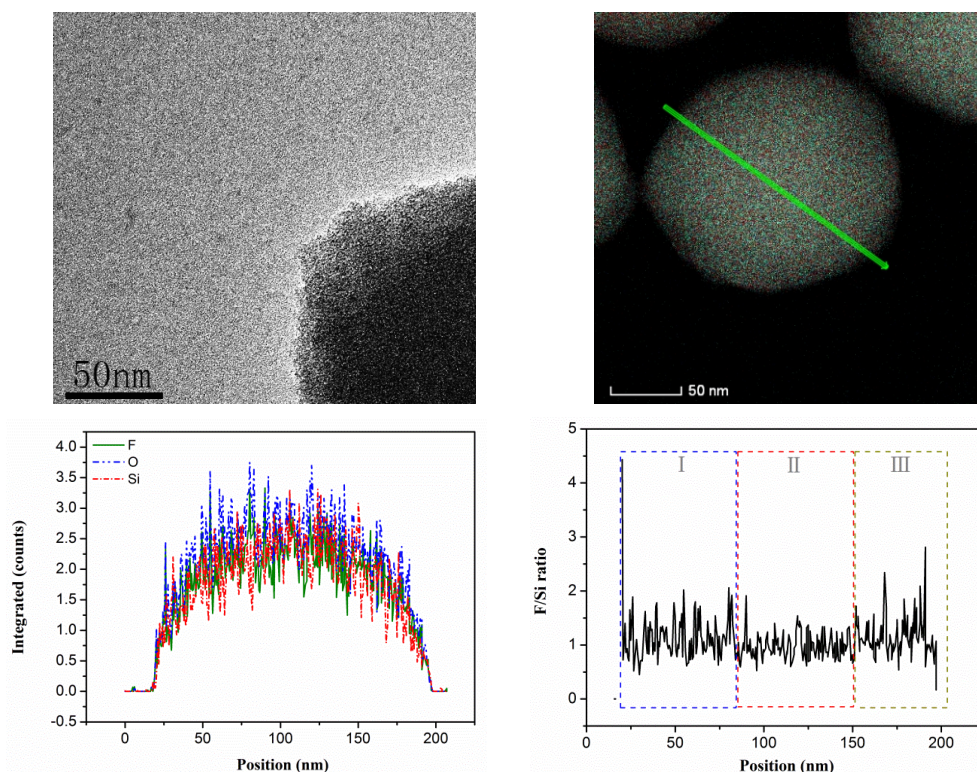
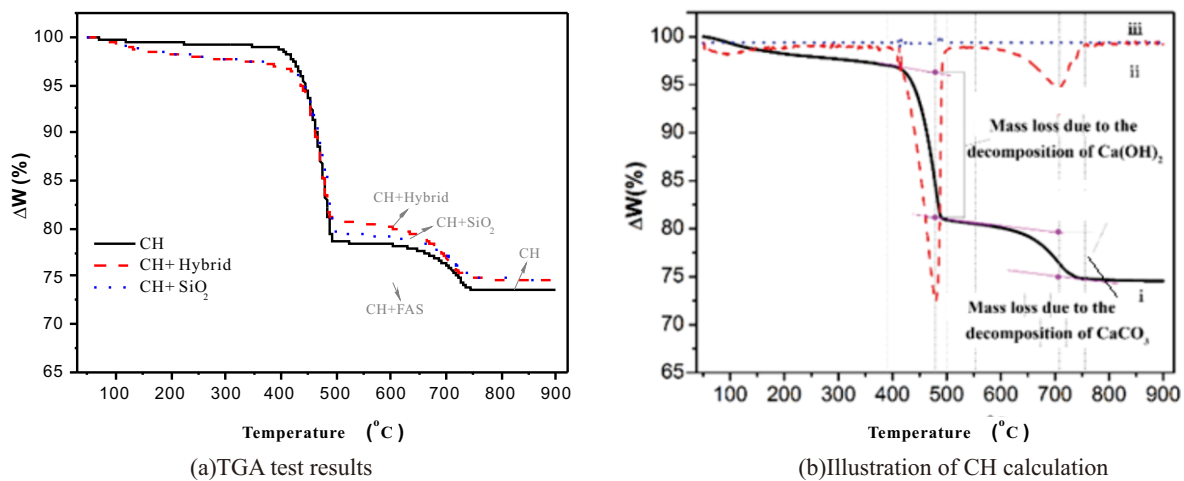


Fig. 2 (a) (b) TEM image of FAS/SiO<sub>2</sub> hybrid material; (c) EDS linear scanning along the diameter of the FAS/SiO<sub>2</sub> hybrid material; (d) F/Si ratio along the diameter of the FAS/SiO<sub>2</sub> hybrid material.



**Fig. 3** TGA curves of FAS/SiO<sub>2</sub>-CH and SiO<sub>2</sub>-CH mixtures.

**Table 2** Normalized CH contents in the FAS/SiO<sub>2</sub>-CH and SiO<sub>2</sub>-CH blends.

Samples	FAS/ SiO <sub>2</sub> -CH-H <sub>2</sub> O	nSiO <sub>2</sub> -CH-H <sub>2</sub> O
CH unconsumed/%	89.44	86.24

Note: the normalization of the CH remaining content was calculated based on the CaO content of the mix after calcination at 900 °C.

**Table 3** The contents of C-S-H gel.

Samples	Mass loss (145°C-350 °C)	C/S	Mass loss (350°C-550 °C)	CH content	Mass loss (600°C-850 °C)	CaCO <sub>3</sub> content
Control1	7.931%	1.030	2.362%	9.715%	3.975%	9.041%
HS-1	4.509%	0.975	3.577%	14.709%	1.808%	4.112%
Control2	7.756%	0.890	3.206%	13.182%	3.912%	8.897%
HS-2	6.558%	0.718	5.747%	23.633%	2.273%	5.169%

quantified by following method developed by Kim [20]. Table 2 lists the normalized CH contents in the tested samples. The amount of CH remained (or consumed) indicates the pozzolanic reactivity of the surface treatment agent with treated concrete.

As seen in Table 3, the unconsumed CH after curing for 3 days was 89.44% and 86.24% for the FAS/SiO<sub>2</sub>-CH-H<sub>2</sub>O sample and nSiO<sub>2</sub>-CH-H<sub>2</sub>O sample, respectively, indicating that the nSiO<sub>2</sub> might have a slightly higher pozzolanic reactivity.

To monitor the interaction of the FAS/SiO<sub>2</sub> hybrid composite and the C-S-H gel on the surface of treated concrete, the chemical and structural features of C-S-H gel were studied. Two types of C-S-H gel with C/S ratios of 1.5 and 1.0 were synthesized, and they were characterized using TGA, as shown in Fig. 4. The purity of C-S-H was determined by TGA and the C/S ratio was calculated according to Foley's research [24] before and after mixing with the FAS/SiO<sub>2</sub> hybrid nanocomposite, and the results are listed in Table 3. As seen from the table, after the hybrid nanocomposite was mixed with the C-S-H gel, the C/S ratio of the both types of C-S-H gel

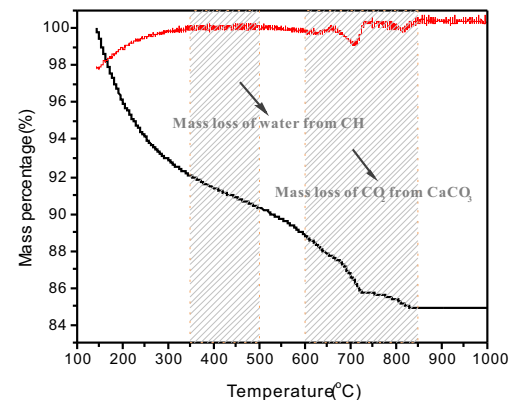


**Fig. 4** TGA curve of C-S-H gel.

decreased from 1.030 and 0.890 to 0.975 and 0.718, respectively. The C/S ratio deduction could be attribute to the reaction of the FAS/SiO<sub>2</sub> hybrid nanocomposite with the synthesized C-S-H gel.

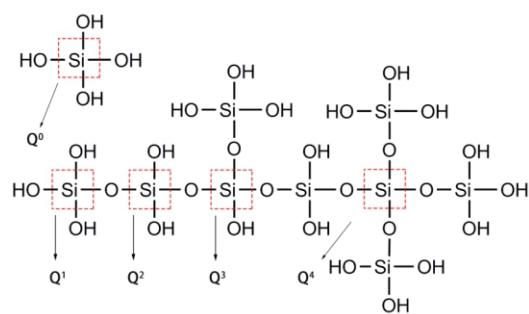


Fig. 5 Schematic representation of a silicate chain of C–S–H gel.

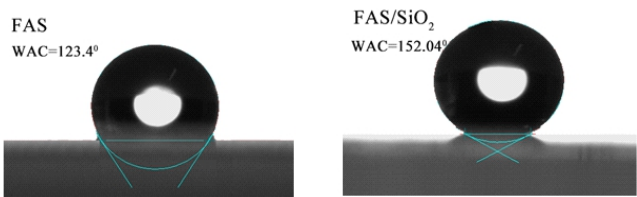


Fig. 7 Water contact angel of FAS andFAS/SiO<sub>2</sub> on glass matrix.

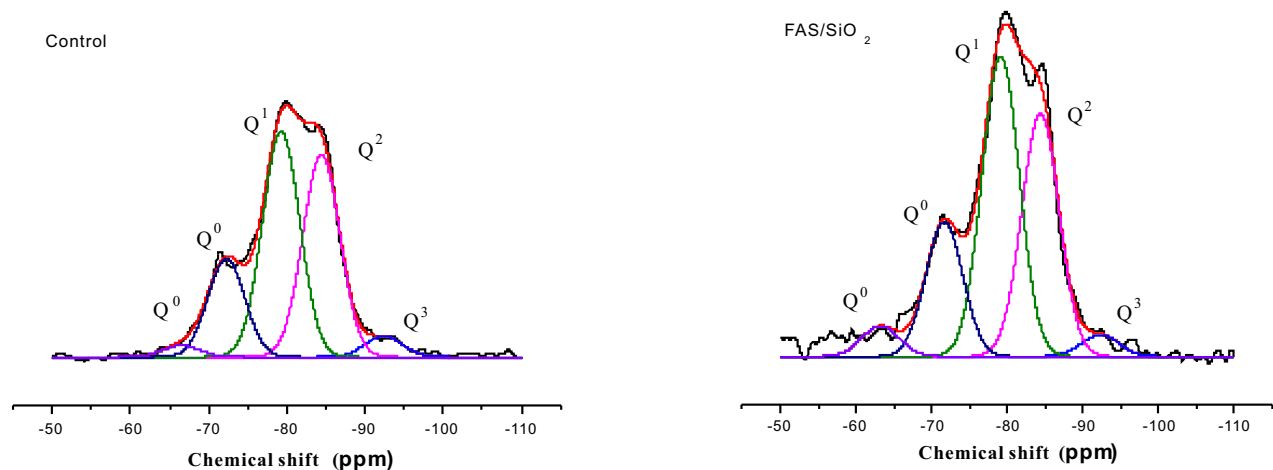


Fig. 6 Deconvolution of the 29SiMAS-NMR spectra of the cement paste before and after treatment (6 month, w/c=0.4).

Table 4 <sup>29</sup>Si MAS NMR analysis of cement paste before and after surface treatment.

	Q0	Q1	Q2	Q3	Q2/Q1	MCL
Control	19.60%	40.44%	36.24%	3.73%	0.896	3.792
FAS/SiO <sub>2</sub>	18.11%	41.15%	37.05%	3.69%	0.900	3.801

The pozzolanic reactivity of the FAS/SiO<sub>2</sub> hybrid nanocomposite and its effect on the C-S-H gel structure were further studied using NMR tests. Fig. 5 shows the schematic representation of a silicate chain of C–S–H gel (n = 1–4). Fig. 6 shows the NMR test results.

The deconvolution of silicate anions of the C-S-H gel was analyzed and the results are listed in Table 4. A slightly increase of Q<sub>2</sub>/Q<sub>1</sub> of the sample can be seen when the FAS/SiO<sub>2</sub> hybrid nanocomposite treatment was applied, indicating the polymerization of the silicate group (the slight increase would be due to the comparably little amount of the hybrid material) during the pozzolanic reaction with cementitious materials.

3.2.2 Hydrophobicity of surface treatment agents

As shown in Fig. 7, the WCA was 123.4 for the FAS-treated sample and the 152.0 for the FAS/SiO<sub>2</sub> hybrid nanocomposite treated sample, indicating that the FAS/SiO<sub>2</sub> hybrid nanocomposite has greater hydrophobicity or superhydrophobicity (WCA>150). This result is comparable to Zhou’s research<sup>15</sup>

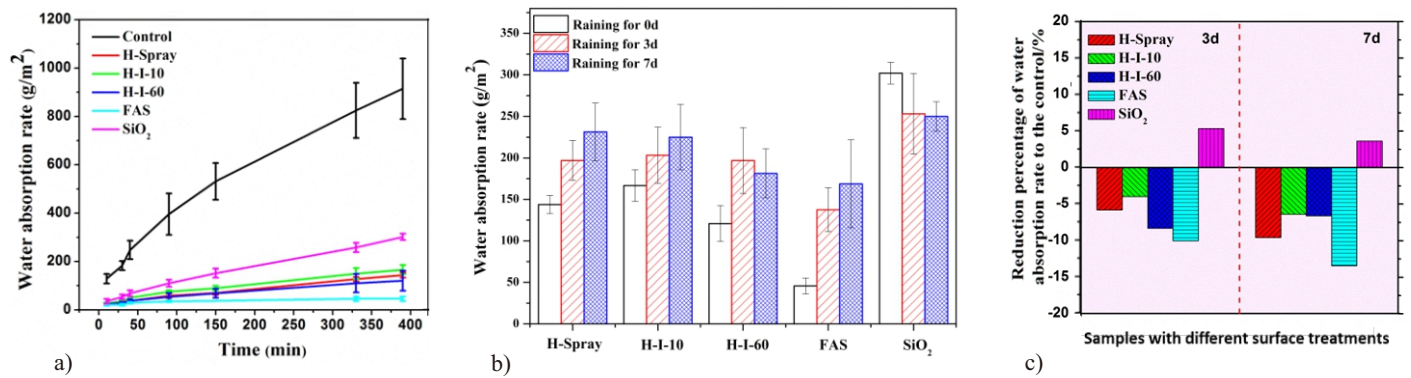
3.3 Properties of surface treated cement-based materials

3.3.1 Water absorption rate

A reduction of the water absorption rate of cementitious material could often lead to an improved durability. Figure. 8a shows the water absorption rate of cement mortar samples treated by different agents after standard curing for 3 days. It can be seen that the hybrid nanocomposite can greatly reduce the water absorption rate compared to that of control samples. The reduction of water absorption rates of the H-Spray-, H-I-10-, H-I-60-, FAS- and SiO<sub>2</sub>-treated samples at 390 soaking time are 84.28%, 81.78%, 86.79%, 94.98% and 66.97% to that of control sample (no surface treatment), respectively.

The hybrid FAS-SiO<sub>2</sub> nanocomposite can reduce the water absorption rate of treated sample much more effectively than the nSiO<sub>2</sub>-treated sample, indicating that the FAS had made a major contribute on the reduction of water absorption rate than nSiO<sub>2</sub>.





(a) Water absorption rate of cement mortar samples treated by various agents, b) water absorption rates of samples before and after raining, c) reduction of water absorption rate after raining-simulation for 3 and 7 days.

**Fig. 8** Results from water absorption rate tests.

After measuring the water absorption rate as shown in Fig. 8a, the samples underwent the detachment test (lab-simulated raining for 3 and 7 days), after which the water absorption rate was measured again (Fig. 8b). The variation of the values of the reduction degree of the water absorption rate to the control sample (un-treated sample) after 3 and 7 days raining to that of sample before raining (Fig. 8a) was compared (Fig. 8c). In the figure, a positive reduction percentage in water absorption rate marks a higher reduction of water absorption rate after raining; while a negative reduction percentage in water absorption rate suggested a lower reduction of water absorption rate after raining, which is due to the detachment of the treatment agent from the surface during raining.

It shows that all the organic agents-treated samples have a negative value after raining, suggesting the detachment of the agents. As the testing time increased from 3 days to 7 days, a decrease in the absolute reduction percentage in water absorption rate indicates a good detachment resistivity of the agent; while an increase in the reduction percentage in water absorption rate signifies the continuous detachment of the agent happens with time.

It can be seen in Fig. 8c that both H-I-60 and SiO<sub>2</sub> treatments improved the detachment resistance of the treatment agents from the cement-based materials. And for H-Spray- and H-I-10- treated samples the reduction of water absorption rate was reduced, but the deterioration ratio is far more less than that of FAS- treated samples, indicating that SiO<sub>2</sub> is beneficial of increasing the bonding of FAS on cement surface.

### 3.3.2 Hydrophobicity of surface treated cement-based materials

The hydrophobicity of the cement paste samples treated by various agents was analyzed and results are shown in Fig. 9, where control sample is the sample with no surface treatment. For H-Spray, H-I-10 and H-I-60-treated samples, the static WCA was hard to determine. Instead, the process of the contact, deformation, and departure of a water droplet (10μL) on the surface of the tested samples was recorded. As seen from Fig. 9a, the water droplet completely departed from the surfaces of cement paste samples treated by H-Spray, H-I-10 and H-I-60 agents. There was no remaining water droplet on the sample surfaces even after significantly elongation of the water drop during this process, indicating the superhydrophobicity of cement-based materials was obtained through the surface treatment.

On the other hand, Fig. 9b shows that the WCA of samples treated by FAS and nSiO<sub>2</sub> agents were only 130.06° and 23.25°, respectively, much lower than the samples treated with the FAS/SiO<sub>2</sub> hybrid nanocomposite (H-spray, H-I-10 and H-I-60). As the hydrophobicity of FAS/SiO<sub>2</sub> hybrid nanocomposite treated samples is greater than that of the FAS treated sample, it implies that the superhydrophobicity of the FAS/SiO<sub>2</sub> hybrid nanocomposite may not ascribe to the organic functional group of the FAS.

### 3.3.3 Roughness

The results and discussions from the previous section (Section 3.3.2) suggest that the chemical group (FAS) may not be the only reason for the superhydrophobicity after surface treatment, which led the study into the surface hierarchical surficial structure of the surface treated cementitious materials as it is another mechanism for achieving superhydrophobicity. According to Wenzel's research,<sup>25</sup> the improvement of the surface roughness could lead to the increase in WCA. For an ideally smooth surface, the relationship between the solid surface and WCA can be explained by Yong's equation,<sup>26</sup> as shown in Eq. (1).

$$\gamma^{sa} = \gamma^{sl} + \gamma^{la} \cos \theta \quad (1)$$

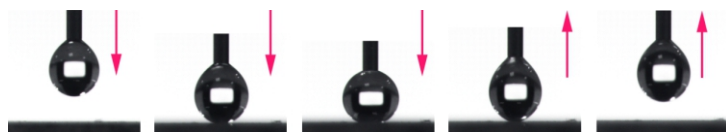
Where  $\gamma^{sa}$ ,  $\gamma^{sl}$  and  $\gamma^{la}$  stand the interfacial tensions of the solid-gas, the solid-liquid, and the liquid-gas interface, respectively, and the  $\theta$  stand for the contact angle of a liquid placed on a flat solid surface, i.e. water contact angle in this situation. However, this equation is not appropriate for an actual surface. Wenzel<sup>25</sup> modified this equation for rough surface, as shown below.

$$\cos \theta_r = \frac{\gamma^{sa} - \gamma^{sl}}{\gamma^{la}} (= r \cos \theta) \quad (2)$$

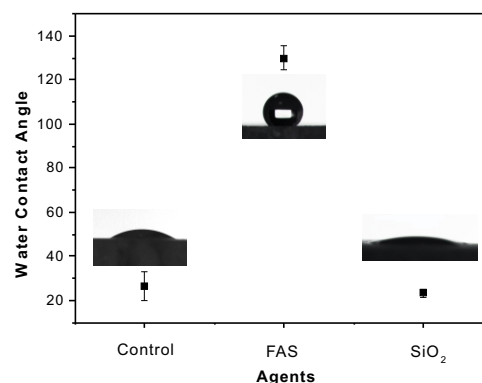
In this equation,  $r$  is a ratio of the actual rough area to the projected area. Through this equation, it is obvious that  $\theta$  can be increased with the increasing of the value of  $r$ , indicating that the increasing of surface roughness contributes to the increasing of water contact angle.

In the present study, the 3D optical profiler was used to capture the roughness of the FAS/SiO<sub>2</sub> hybrid nanocomposite treated cement paste surfaces, and the results are shown in Figs. 10&11. The figures

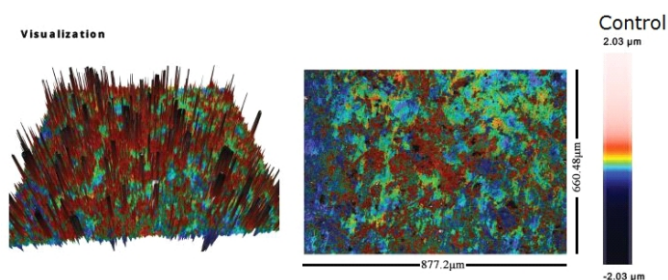
**Fig. 9** Illustration of the measurement and WCA of surface treated cement paste samples.



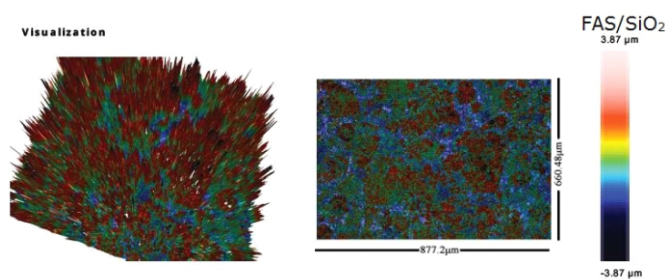
(a) Water droplet movement on the surface of samples treated with hybrid FAS/SiO<sub>2</sub> nanocomposite (H-spray, H-I-10 and H-I-60).



(b) WCA of cement paste samples treated by different surface treatment agents.



(a) Control sample (no surface treatment/before treatment).



(b) Sample treated with the FAS/SiO<sub>2</sub> hybrid nanocomposite.

**Fig. 10** 3D roughness image of cement paste surface before and after treatment.

show that the surface roughness increased by all surface treatment agents used, especially by the hybrid FAS/SiO<sub>2</sub> hybrid nanocomposite, from 0.231 (no surface treatment) to 1.086 (FAS/SiO<sub>2</sub> hybrid nanocomposite treated). Such a significant increase in surface roughness might have considerably contributed to the increase in WCA of the surface treated cementitious materials.

### 3.3.4 Surface morphology

The morphology of the surface-treated cement pastes at an age of 3 days were examined under SEM. The sample surface was observed. As shown in Fig. 12a, many cubic-like crystals were seen in the control sample (with no surface treatment), which were confirmed to be CaCO<sub>3</sub> crystals by EDS. Fig. 12b displays needle-shaped crystal clusters. Fig. 12c exhibits the adsorption of nSiO<sub>2</sub> on the surface of the sample. And this is same as the filling of the porous structure of cement concrete with nanoparticles.<sup>27</sup> Fig. 12(d) illustrates that morphology of the surface of the FAS/SiO<sub>2</sub> hybrid agent treated sample clearly distinguished itself from all the samples above. Little/no cubic and rod-shaped crystals were clearly seen but mass nano-sized were observed. These particles appeared less clustered, less spherical, and smaller than those seen in Figure. 12c, the sample treated with nSiO<sub>2</sub>, which might have helped increase the surface roughness of the FAS/ nSiO<sub>2</sub> treated sample.

Hierarchical structure was also found on the surface of cement paste samples treated by FAS/SiO<sub>2</sub> hybrid nanocomposite: it can be seen in Fig. 13 that nanoparticles adhere to the surface of the micron grains of the hydration products of cement, which could significantly improve the hydrophobicity acquiring superhydrophobic surface.<sup>28</sup>

### 3.4 Durability of cement-based material after treated by FAS/SiO<sub>2</sub> hybrid materials

Based on the discussion above, the superhydrophobic surface of existing concrete structures can be acquired easily through FAS/SiO<sub>2</sub> treatment. A critical issue is whether the treatment agent could have a good bond with the treated concrete and good resistance to weathering during its service time. Since organic compounds are likely to deteriorate under a UV aging process, the aging resistance of the surface treatment agents containing organic components (e.g., HS, FAS, and FAS/SiO<sub>2</sub>) were exposed to UV radiation. In the test, the WCA of the tested samples were measured at different times of UV exposure, and the results are shown in Fig. 14.

As seen in Figure. 14, FAS/SiO<sub>2</sub> treated sample shows superior hydrophobicity, with the highest WCA values among the tested samples at all ages, especially during the first 70 radiation hours. (As indicated in Fig. 9(a), the static WCA was unable to record. As the UV radiation time increased, the WCA decreased, indicating the degradation of organic component of the surface treatment agents. Regardless the decreasing trend, the results show that the WCA of the FAS/SiO<sub>2</sub> sample was still 120° after 800 hours UV radiation. It can also be found that the WCA of sample treated by HS is lower than that of FAS/SiO<sub>2</sub> and FAS treated sample, and the value is fluctuated, indicating that the effect of samples treated by immersing in hybrid solution is better than spraying method. That is, the immersing method is more effective.

### Conclusions

In this work, a novel FAS/SiO<sub>2</sub> hybrid nanocomposite was designed



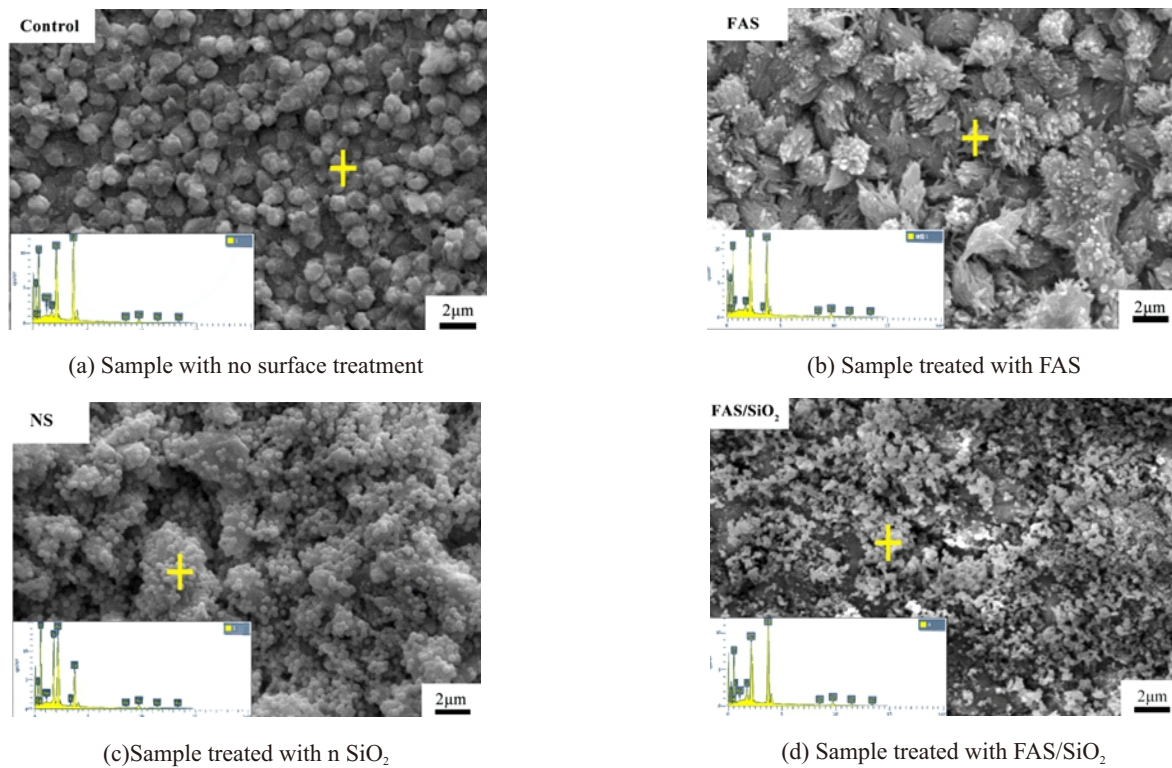


**Fig. 12** Surface morphology of cement pastes with different surface treatments.

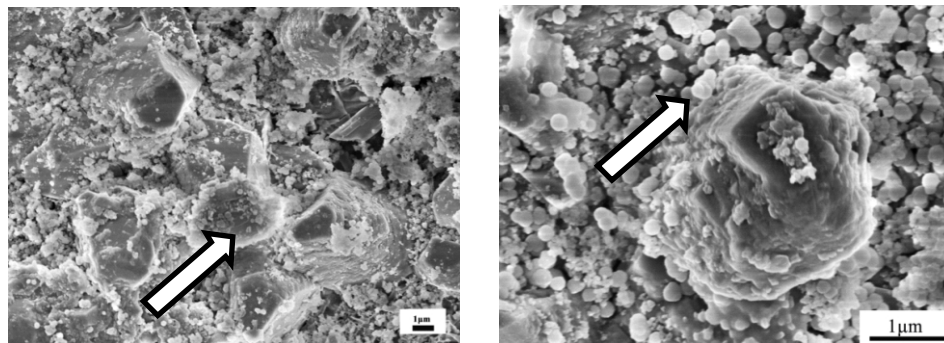


**Fig. 13** Hierarchical structure of the FAS/SiO<sub>2</sub>-treated cement paste.

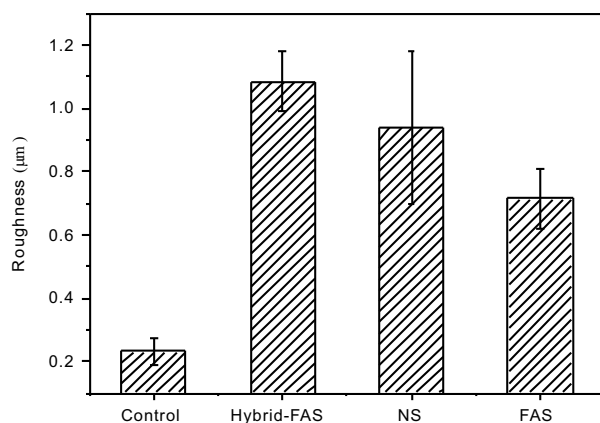


**Fig. 11** The surface roughness of cement paste sample after treated by different agents.

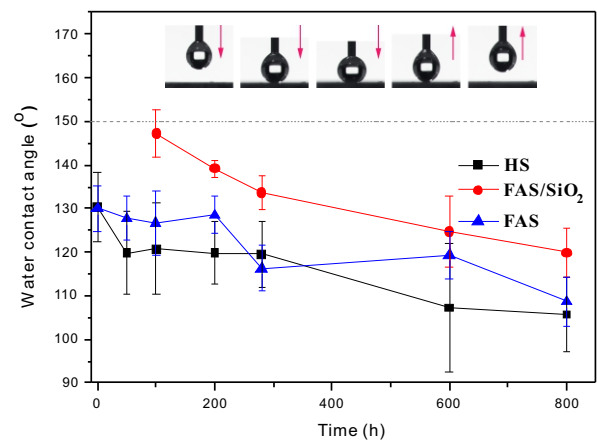


**Fig. 14** Water contact angle of cement paste samples treated by various agents after UV test aging.

and synthesized for surface treatment of hardened cementitious materials. The characteristic of the nanocomposite and their effects on WCA and water absorption rate were investigated, and the reaction mechanisms were discussed. The following conclusion can be drawn:

1. When used as a surface treatment agent for a hardened cement-based material, the FAS/SiO<sub>2</sub> hybrid nanocomposite synthesized endowed superhydrophobicity to the surface of the treated material.

2. The FAS/SiO<sub>2</sub> hybrid nanocomposite could reduce the water absorption rate of the treated concrete materials significantly, and it showed great anti-detachment performance under rain-simulation, which provides a high potential for extending service life of field concrete materials.

3. Under the UV aging test, the FAS/SiO<sub>2</sub> hybrid material exhibited good durability, and the surface of the FAS/SiO<sub>2</sub> treated cement paste samples was still hydrophobic after 800 hours of the UV lighting test.

This work has suggested that taking advantages of both organic and inorganic silica-based treatment agents that have already been used in practice, the hybrid nanocomposite demonstrated synergic effects on its key engineering properties (e.g., hydrophobicity, water absorption rate, detachment resistance, and durability). This approach could serve as an example for future development of new types of surface treatment agents for cement-based materials.

## Acknowledgement

The authors gratefully acknowledge the financial support from National Key R&D Plan (2016YFE0206100), Natural Science Foundation of China (Grants No. 51672107 and 51761145023), and the 111 Project of International Corporation on Advanced Cement-based Materials (No. D17001) and Shenzhen Gangchuang Building Material Co., Ltd.

## Reference

1. V. Papadakis, A. Roumeliotis, M. Fardis and C. Vagenas, Proceedings of the International Conference, 1996, 165-174.
2. S. Kosmatka, B. Kerkhoff and W. Panarese, *Design and Control of Concrete Mixtures*, 14th edn., Association Canadienne du Ciment Portland, 2002.
3. N. M. Al-Akhras, *Cem. Concr. Res.*, 2006, **36**, 1727-1734.
4. J. Liu, Q. Qiu, X. Chen, F. Xing, N. Han, Y. He and Y. Ma, *Cem. Concr. Res.*, 2017, **95**, 217-225.
5. H. Cai and X. Liu, *Cem. Concr. Res.*, 1998, **28**, 1281-1287.
6. H. S. Shang, Y. P. Song and L. K. Qin, *Build. Environ.*, 2008, **43**, 1197-1204.
7. Y. Zhu, S. Kou, C. Poon, J. Dai and Q. Li, *Cem. Concr. Compos.*, 2013, **35**, 32-38.
8. S. Muzenski, I. Flores-Vivian and K. Sobolev, *Cem. Concr. Compos.*, 2015, **57**, 68-74.
9. H. Li, X. Zhao, G. Chu, S. Zhang and X. Yuan, *RSC Adv.*, 2014, **4**, 62694-62697.
10. P. Liu, Y. Gao, F. Wang, J. Yang, X. Yu, W. Zhang and L. Yang, *J. Cleaner Prod.*, 2017, **156**, 775-785.
11. R. San Nicolas, S. A. Bernal, R. Mejía de Gutiérrez, J. S. J. van Deventer and J. L. Provis, *Cem. Concr. Res.*, 2014, **65**, 41-51.
12. Y. Cai, P. Hou, C. Duan, R. Zhang, Z. Zhou, X. Cheng and S. Shah, *Constr. Build. Mater.*, 2016, **117**, 144-151.
13. P. Y. Dan Wang, Pengkun Hou, Lina Zhang, Zonghui Zhou, Xin Cheng, *Cem. Concr. Res.*, 2016, **87**, 22-30.
14. P. Hou, J. Qian, X. Cheng and S. P. Shah, *Cem. Concr. Compos.*, 2015, **55**, 250-258.
15. H. Zhou, H. Wang, H. Niu, A. Gestos, X. Wang and T. Lin, *Adv. Mater.*, 2012, **24**, 2409-2412.
16. M. Z. Guo, A. Maury-Ramirez and S. P. Chi, *Build. Environ.*, 2015, **94**, 395-402.
17. W. Guan, F. Ji, Z. Fang, D. Fang, Y. Cheng, P. Yan and Q. Chen, *Ceram. Int.*, 2014, **40**, 4415-4420.
18. Y. He, X. Zhao, L. Lu, L. J. Struble and S. Hu, *Journal of Wuhan University of Technology, Mater. Sci. Ed.*, 2011, **26**, 770-773.
19. I. Standards, Geometrical Product Specifications (GPS): Surface Texture: Profile Method: Terms, Definitions and Surface Texture Parameters, 1997, ISO 4287:1997.
20. T. Kim and J. Olek, *Transp. Res. Rec.*, 2012, 2290, 10-18.
21. W. Wu, H. Chen, C. Liu, Y. Wen, Y. Yuan and Y. Zhang, *Colloids Surf., A*, 2014, **448**, 130-139.
22. R. Li, P. Hou, N. Xie, Z. Ye, X. Cheng and S. P. Shah, *Cem. Concr. Compos.*, 2018, **87**, 89-97.
23. B. Qiao, T. Wang, H. Gao and Y. Jin, *Appl. Surf. Sci.*, 2015, **351**, 646-654.
24. E. Foley, J. Kim, M. Taha, *Cem. Concr. Res.*, 2012, **42**, 1225-1232.
25. R. N. Wenzel, *J. Phys. Colloid Chem.*, 1949, **53**, 1466-1467.
26. Y. Tomas, *Philos. Trans. R. Soc. London*, 1804, **95**, 65-87.
27. S. Ghahari, E. Ghafari, N. Lu, *Constr. Build. Mater.*, 2017, **146**, 755-63.
28. T. Verho, C. Bower, P. Andrew, S. Franssila, O. Ikkala and R. H. Ras, *Adv. Mater.*, 2011, **23**, 673-678.